

## Supporting Information

# **A High Loaded Catalyst of Highly Dispersed Nickel Species on Acid-Treated Mesoporous Clay Layers for Efficient CO and CO<sub>2</sub> Methanation**

Feifei Li <sup>a</sup>, Junbo Zhang <sup>a</sup>, Yufu Liu <sup>a</sup>, Guanjun Gao <sup>a</sup>, Yi He <sup>a</sup>, and Xuzhuang Yang <sup>a</sup>,

<sup>b\*</sup>

<sup>a</sup> College of Chemistry and Chemical Engineering, Inner Mongolia University, Hohhot 010021, China

<sup>b</sup> Inner Mongolia Key Lab of Rare Earth Materials Chemistry and Physics, Inner Mongolia University, Hohhot, Inner Mongolia, 010021, P. R. China;

\*Corresponding author: Xuzhuang Yang

E-mail address: [xzyang@imu.edu.cn](mailto:xzyang@imu.edu.cn)

---

## 1. Orthogonal experimental design.

To screen catalysts, we investigated the effects of four factors: (1) two types of clays, raw montmorillonite (A0) and acid-modified montmorillonite (A1); (2) four nickel loadings of 5% (B5), 10% (B10), 15% (B15), and 20% (B20); (3) four types of amino acids, L-lysine (C1), L-alanine (C2), L-serine (C3), and glycine (C4); and (4) four amino acid to nickel molar ratios of 0 (D0), 1 (D1), 2 (D2), and 3 (D3). Table S1 illustrates the orthogonal experimental scheme created by the statistical program Statistical Product and Service Solutions (SPSS).

**Table S1** Orthogonal experimental scheme

Catalysts	Clays	Ni loadings	Amino acids	Molar ratio
1	A0	B10	C1	D1
2	A1	B20	C1	D3
3	A1	B15	C1	D2
4	A0	B5	C3	D3
5	A0	B20	C2	D1
6	A1	B10	C4	D0
7	A0	B15	C4	D3
8	A0	B15	C2	D0
9	A0	B10	C3	D2
10	A0	B20	C4	D2
11	A1	B20	C3	D0
12	A0	B5	C1	D0
13	A1	B15	C3	D1
14	A1	B5	C4	D1
15	A1	B10	C2	D3
16	A1	B5	C2	D2

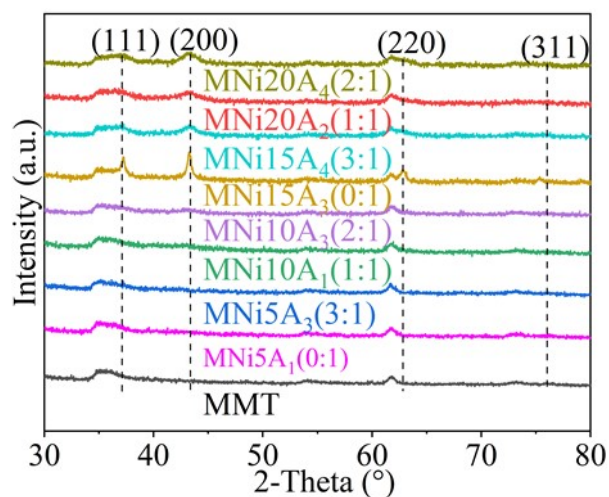


**Fig. S1.** XRD patterns of nickel catalysts supported on the M (MNiA<sub>b</sub>(D))

**Table S2** The amount of Ni in the catalyst and the size of NiO particles

Catalyst	Ni loading (wt.%)	NiO particle size (nm)
MNi5A <sub>1</sub> (0:1)	5	-
MNi5A <sub>3</sub> (3:1)	5	-
MNi10A <sub>1</sub> (1:1)	10	-
MNi10A <sub>3</sub> (2:1)	10	-
MNi15A <sub>3</sub> (0:1)	15	56.32
MNi15A <sub>4</sub> (3:1)	15	13.36
MNi20A <sub>2</sub> (1:1)	20	9.28
MNi20A <sub>4</sub> (2:1)	20	15.94

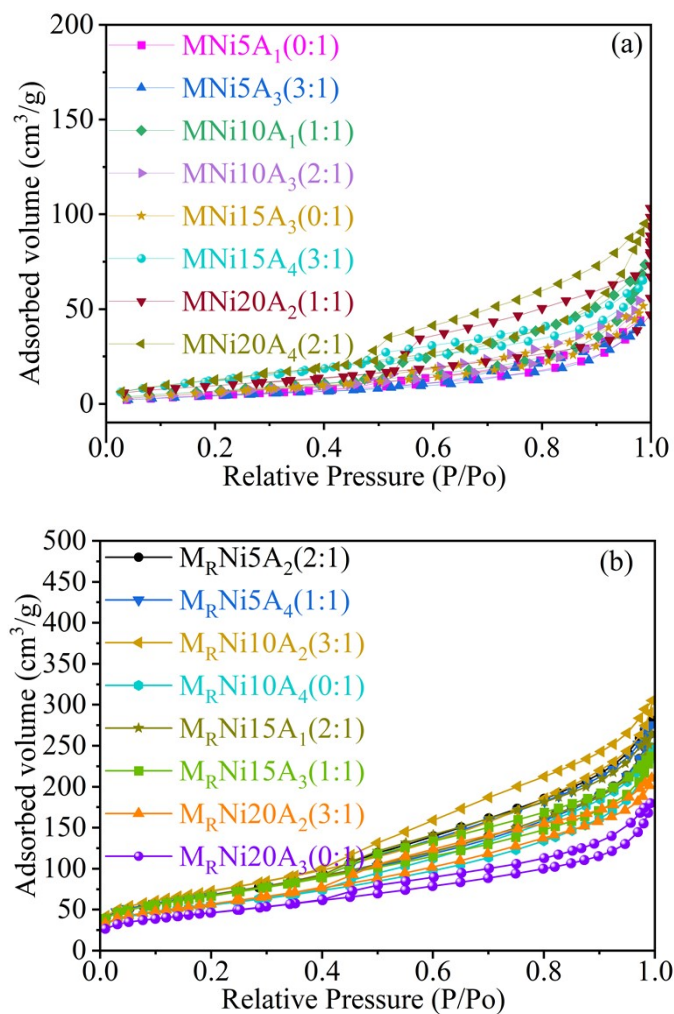


**Fig. S2.**  $N_2$  adsorption-desorption isotherms and pore size distribution curves of (a, b) the catalysts designed for orthogonal experiment

---

## 2.Catalyst activity

**Table S3** Orthogonal experiment CO conversion, CH<sub>4</sub> selectivity, and formation rate for the CO methanation

Catalysts	Factor				CO Conv. (%)	S <sub>CH<sub>4</sub></sub> (%)	Formation rate (%)
	A	B	C	D			
1	0	10	1	1	98.8	75.3	74.2
2	1	20	1	3	99.5	78.7	78.2
3	1	15	1	2	99.7	79.7	79.3
4	0	5	3	3	83.0	76.8	51.2
5	0	20	2	1	99.7	81.2	80.9
6	1	10	4	0	98.4	72.4	69.9
7	0	15	4	3	99.5	77.7	77.2
8	0	15	2	0	98.5	73.9	72.8
9	0	10	3	2	99.0	75.7	74.9
10	0	20	4	2	99.7	81.0	80.8
11	1	20	3	0	98.9	76.4	75.6
12	0	5	1	0	71.5	62.8	44.8
13	1	15	3	1	99.5	79.4	79.0
14	1	5	4	1	94.5	69.0	64.9
15	1	10	2	3	98.5	73.4	71.9
16	1	5	2	2	92.6	67.7	62.7

---

**Table S4** CO conversion range analysis data for the CO methanation

Value name	A	B	C	D
K1	93.7	85.4	92.2	91.8
K2	97.6	98.7	97.3	98.1
K3		99.3	95.1	97.8
K4		99.2	91.8	94.9
Rj	3.9	13.9	5.9	6.3
Importance		B>D>C>A		

**Table S5** CH<sub>4</sub> Selectivity range analysis data for the CO methanation

Value name	A	B	C	D
K1	73.9	65.9	74.1	71.4
K2	74.6	74.2	74.0	76.2
K3		77.7	73.9	76.0
K4		79.3	75.0	73.5
Rj	0.6	13.5	0.9	4.9
Importance		B>D>C>A		

**Table S6** CH<sub>4</sub> Formation Rate range analysis data for the CO methanation

Value name	A	B	C	D
K1	69.6	55.9	69.1	65.7
K2	72.7	72.7	72.1	74.8
K3		77.0	70.2	74.4
K4		78.9	73.2	69.6
Rj	3.1	22.9	4.1	9.0
Importance		B>D>C>A		

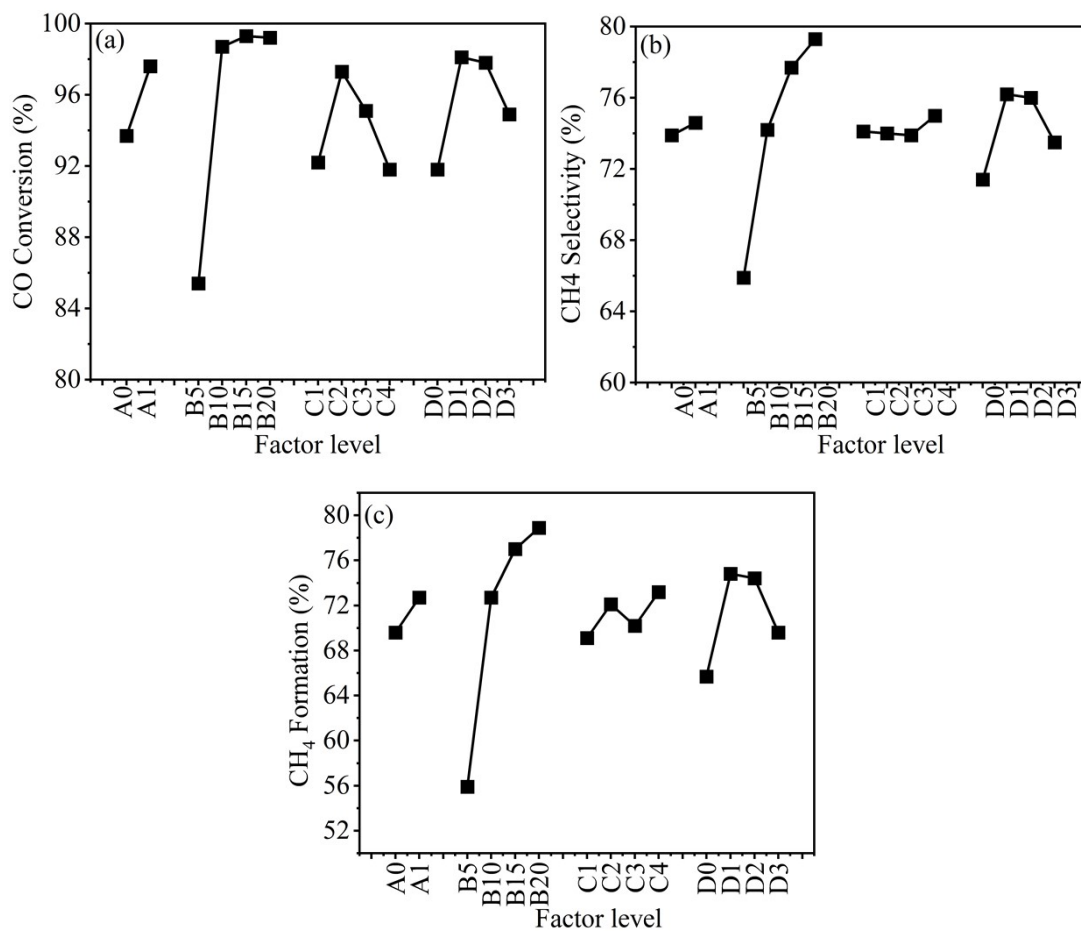


**Fig. S3.** Factor level diagram for the CO methanation.

**Table S7** Orthogonal experiment CO<sub>2</sub> conversion, CH<sub>4</sub> selectivity, and formation rate for the CO<sub>2</sub> methanation

Catalysts	Factor				CO <sub>2</sub> Conv. (%)	S <sub>CH4</sub> (%)	Formation rate (%)
	A	B	C	D			
1	0	10	1	1	82.1	99.1	81.2
2	1	20	1	3	88.4	99.5	87.9
3	1	15	1	2	88.0	99.6	87.6
4	0	5	3	3	64.3	93.8	60.3
5	0	20	2	1	89.5	99.6	89.1
6	1	10	4	0	76.0	97.0	72.9
7	0	15	4	3	84.0	99.3	83.2
8	0	15	2	0	77.0	98.5	75.5
9	0	10	3	2	78.0	98.3	76.4
10	0	20	4	2	88.4	99.6	88.1
11	1	20	3	0	83.8	99.3	82.9
12	0	5	1	0	60.4	90.8	54.8
13	1	15	3	1	88.0	99.5	87.1
14	1	5	4	1	66.0	94.0	62.0
15	1	10	2	3	80.8	98.9	79.6
16	1	5	2	2	72.5	95.9	69.1

**Table S8** CO<sub>2</sub> conversion range analysis data for the CO<sub>2</sub> methanation

Value name	A	B	C	D
K1	77.9	67.1	79.8	77.3
K2	81.1	79.2	79.9	82.7
K3		84.3	78.5	81.7
K4		87.5	79.9	79.4
Rj	3.1	20.5	1.4	5.3
Importance		B>D>A>C		

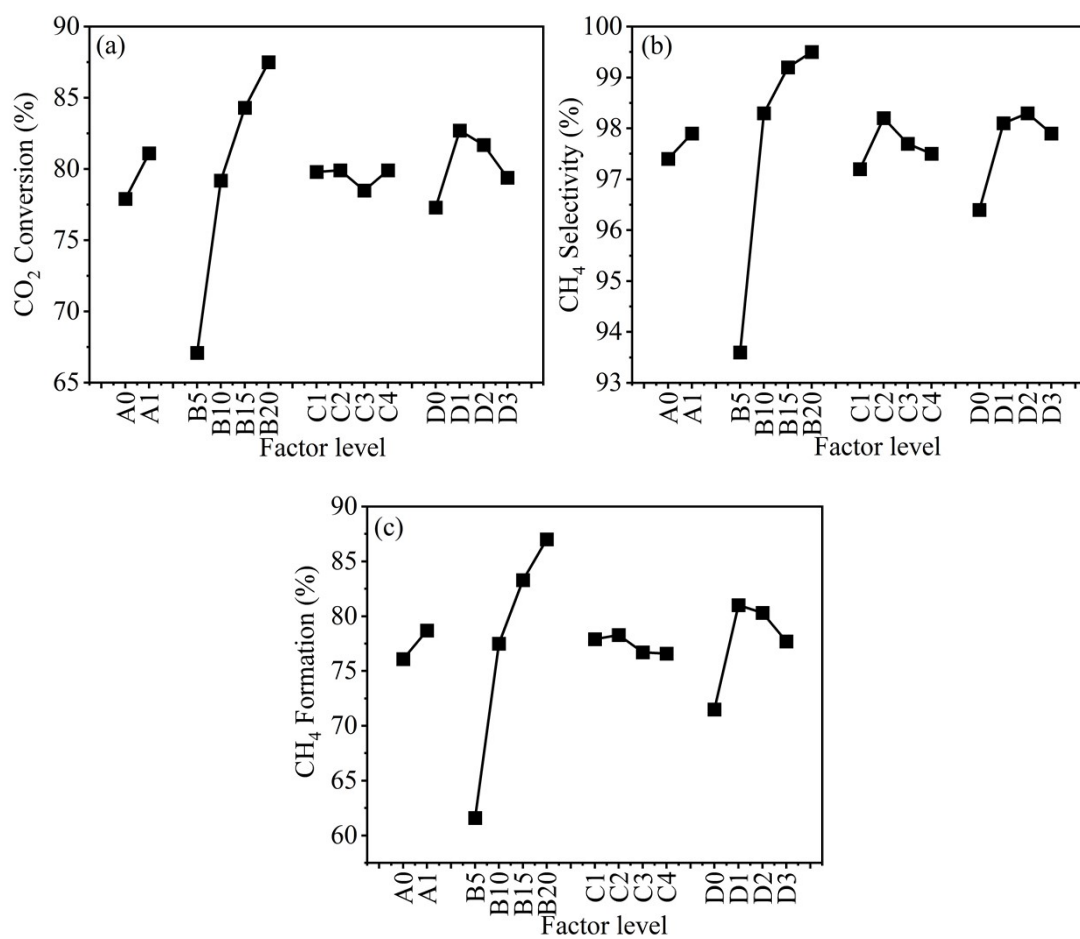
**Table S9** CH<sub>4</sub> Selectivity range analysis data for the CO<sub>2</sub> methanation

Value name	A	B	C	D
K1	97.4	93.6	97.2	96.4
K2	97.9	98.3	98.2	98.1
K3		99.2	97.7	98.3
K4		99.5	97.5	97.9
Rj	0.6	5.9	0.9	1.9
Importance		B>D>C>A		

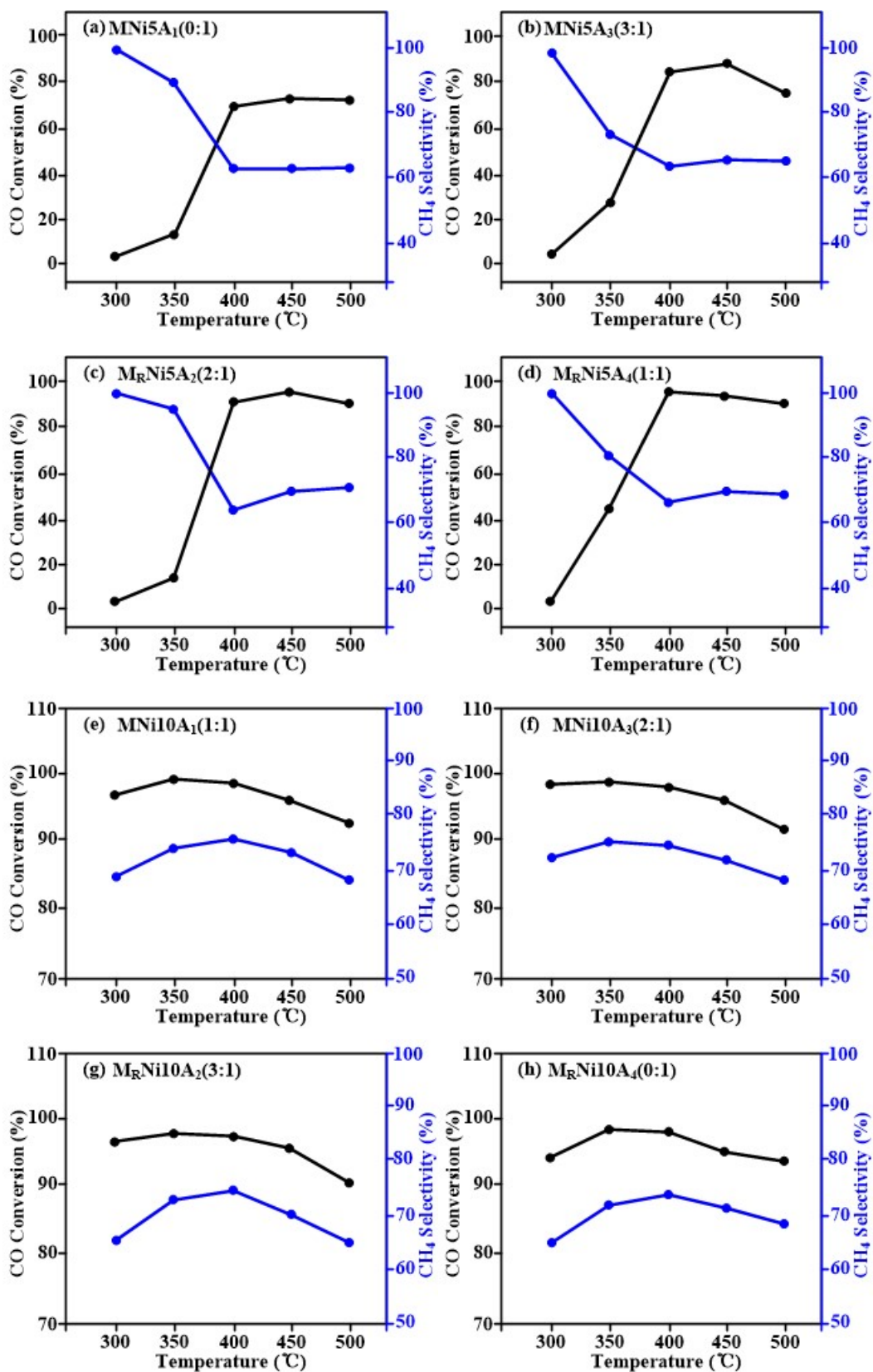


**Table S10** CH<sub>4</sub> Formation Rate range analysis data for the CO<sub>2</sub> methanation

Value name	A	B	C	D
K1	76.1	61.6	77.9	71.5
K2	78.7	77.5	78.3	81.0
K3		83.3	76.7	80.3
K4		87.0	76.6	77.7
Rj	2.6	25.4	1.8	9.5
Importance	B>D>A>C			



**Fig. S4.** Factor level diagram for the CO<sub>2</sub> methanation.



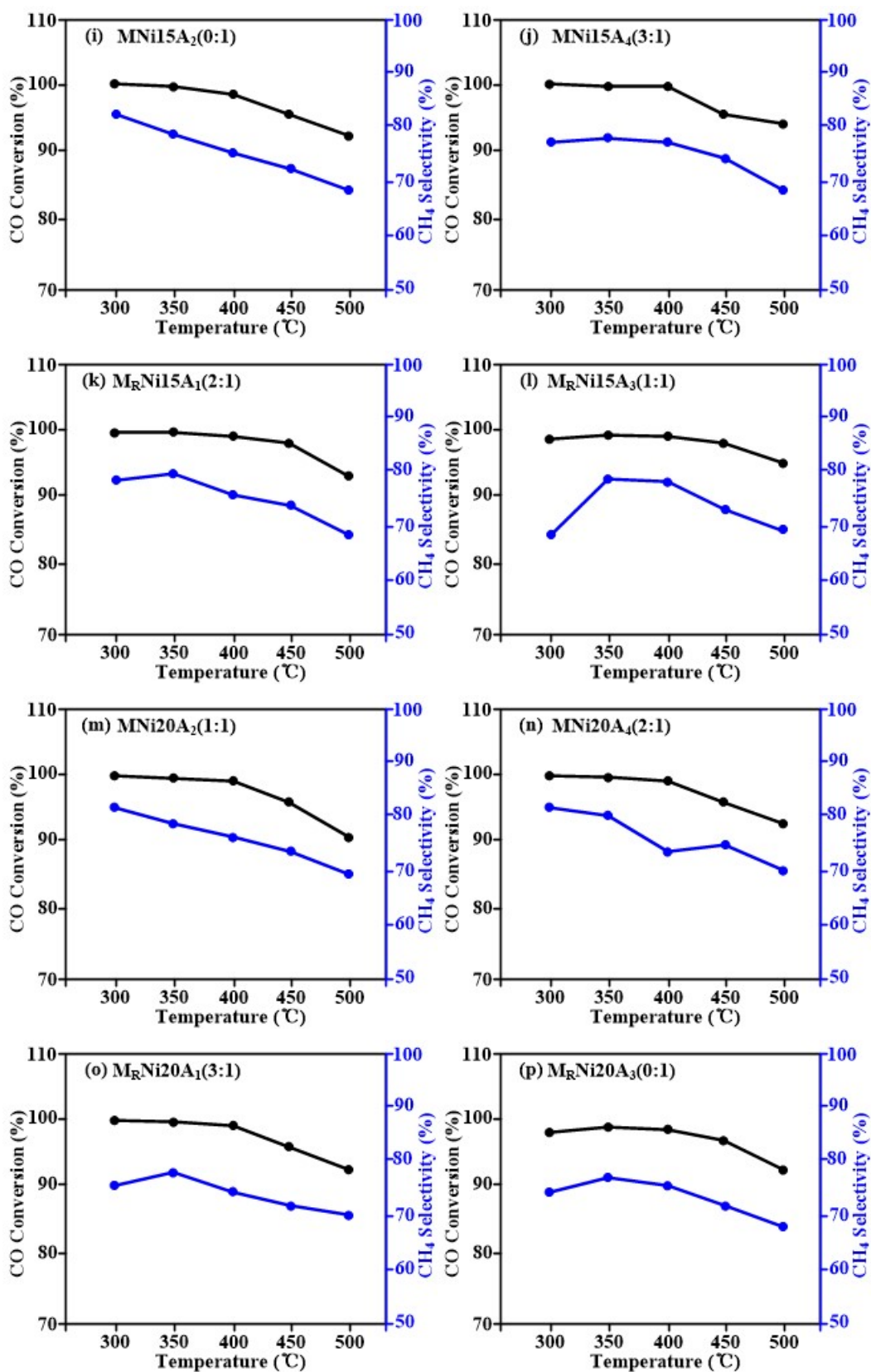
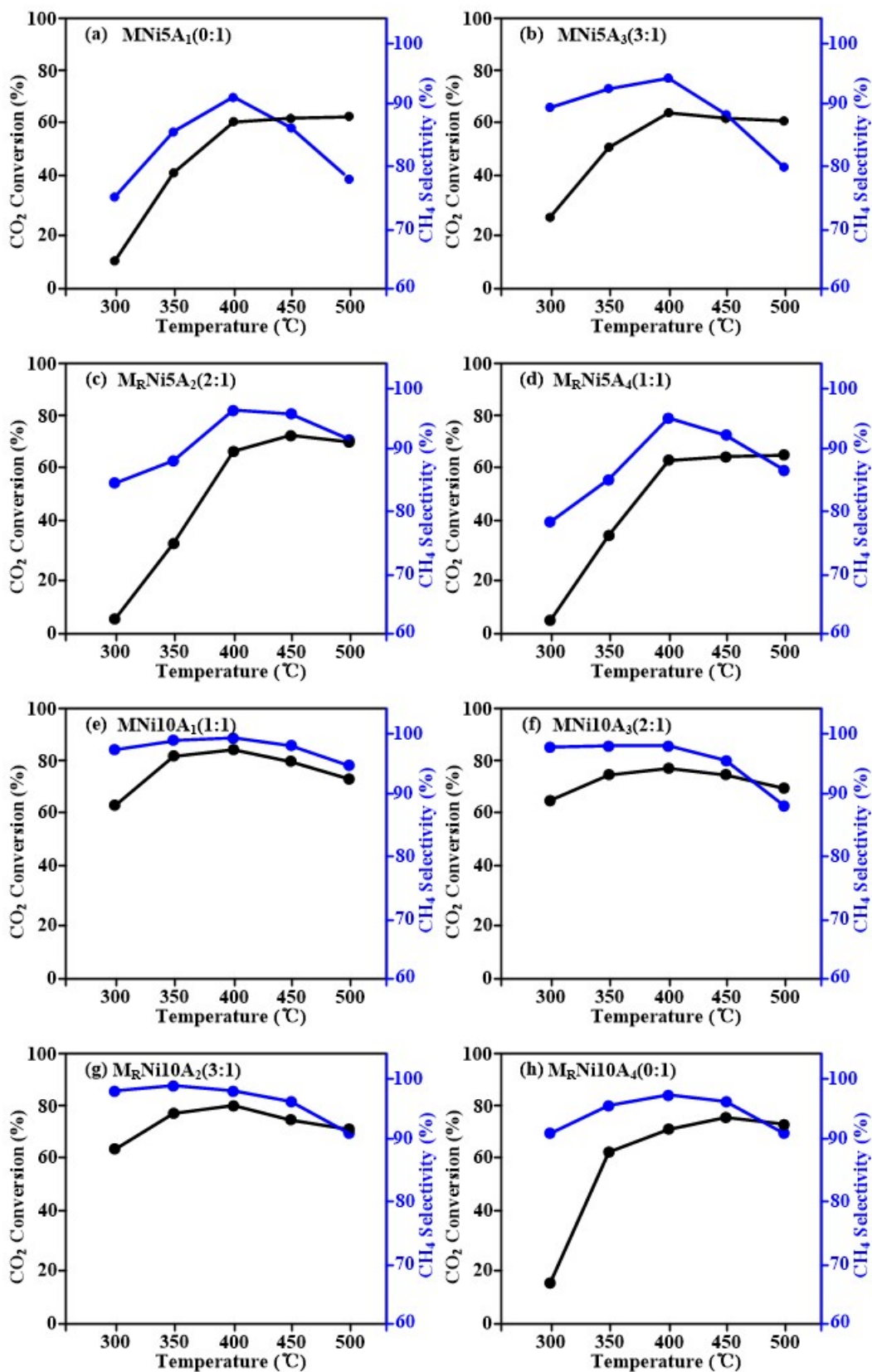


Fig. S5. CO Conversion and CH<sub>4</sub> selectivity of different catalysts for CO methanation.



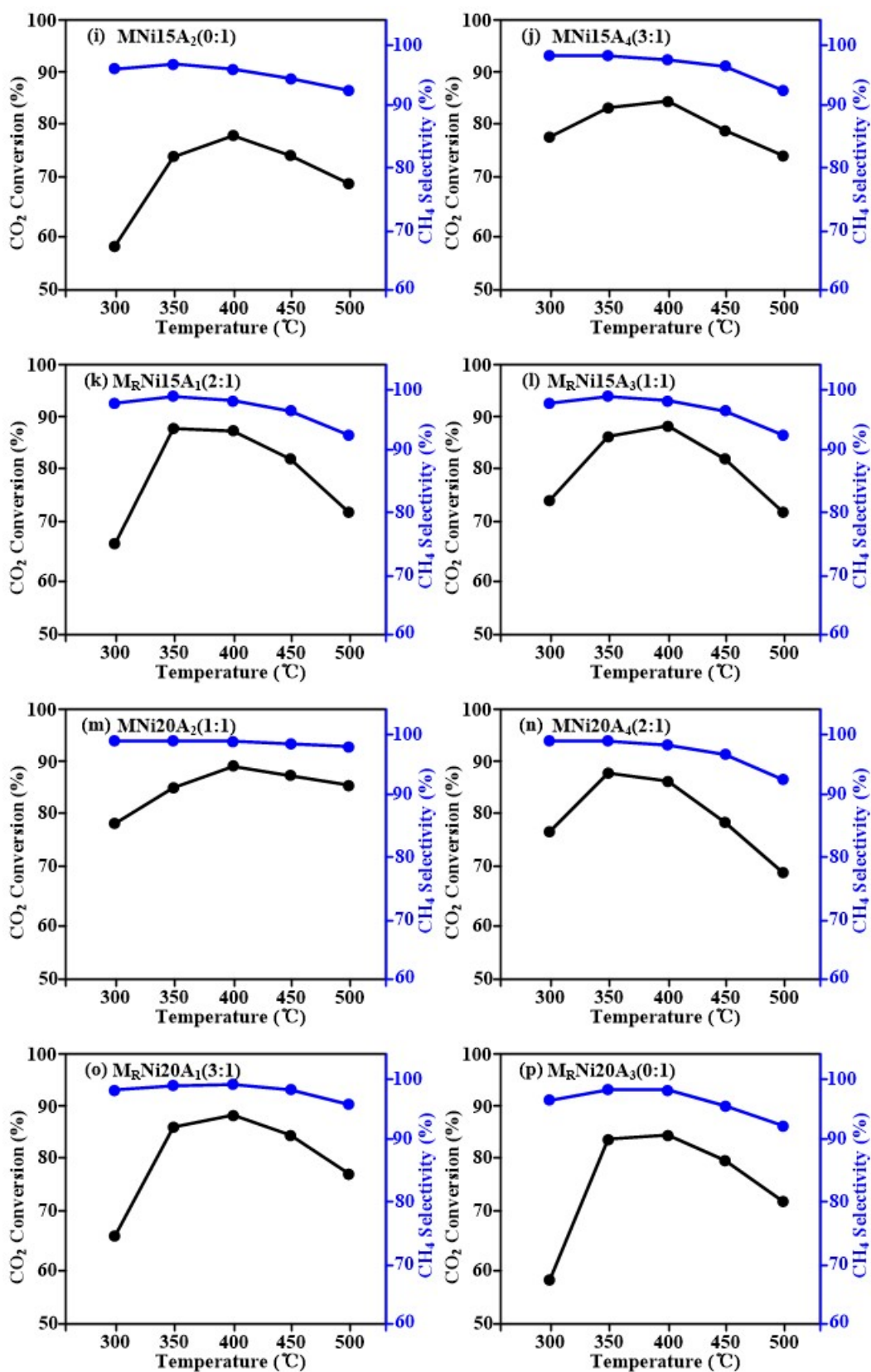
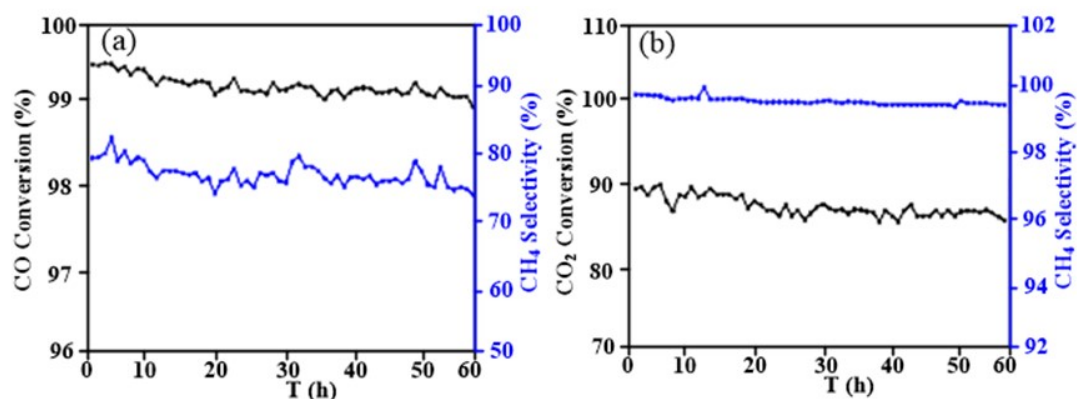


Fig. S6. CO<sub>2</sub> Conversion and CH<sub>4</sub> selectivity of different catalysts for CO<sub>2</sub> methanation.



### 3. Stability



**Fig. S7.** Time on steam of the catalyst of MNi<sub>20</sub>A<sub>2</sub>(1:1) (a) CO methanation and (b) CO<sub>2</sub> methanation. GHSV= 12000 h<sup>-1</sup>, 0.1MPa and T= 400 °C for CO methanation; GHSV= 15000 h<sup>-1</sup>, 0.1 MPa and T= 400 °C for CO<sub>2</sub> methanation.

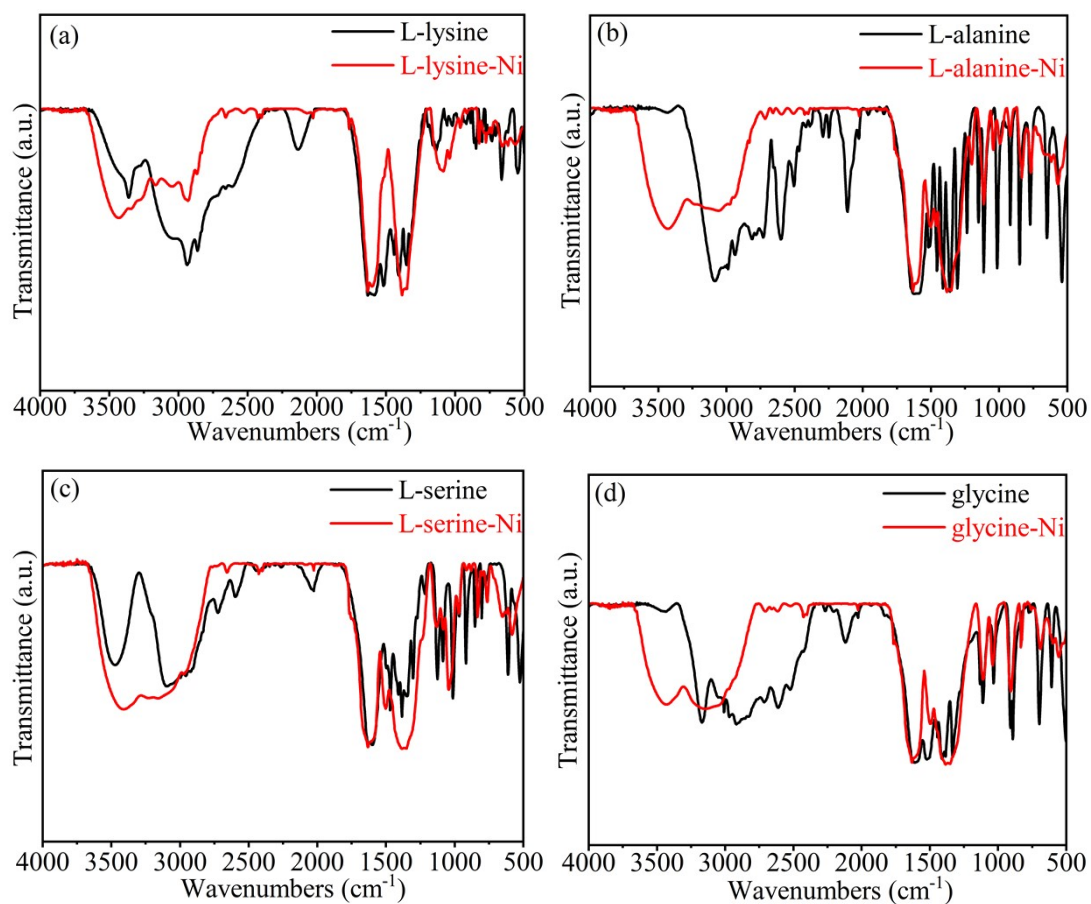


**Fig. S8.** FT-IR spectra of the samples (a) L-lysine, L-lysine-Ni, (b) L-alanine, L-alanine-Ni, (c) L-serine, L-serine-Ni, (d) glycine, glycine-Ni.